In this study, rat CPB was also maintained under nonphysiological hyperoxic conditions as used in clinical CPB. Lee and Choi (25) previously showed that hyperoxia induces oxidative cell damage by promoting the formation of ROS and the expression of inflammatory cytokines (25). Therefore, it is highly likely that hyperoxia contributed partly to the increase in the serum cytokine and biochemical markers in our rat CPB model. Hence, H_2 insufflation may attenuate the hyperoxia-induced formation of ROS and cytokines through the antioxidant effects.

It is generally known that hemolysis is induced by mechanical stress during CPB (26). Therefore, it is possible that biochemical markers (LDH, AST, and ALT) were not reduced in CPB to the level observed in SHAM rats in part because H_2 insufflation does not reduce the mechanical stress-induced increase in hemolysis.

The present study showed that the W/D ratio of the lung increased during CPB. These data are consistent with a previous study (27) that showed an increase in the W/D ratio of the lung and pulmonary edema in a rat CPB model. Our new finding is that this increase in the W/D ratio was attenuated with H_2 insufflation. Because CPB increases pulmonary vascular permeability (28), it is possible that H_2 insufflation attenuates the injury of pulmonary vascular endothelium by scavenging ROS and reducing the increase in vascular permeability during CPB.

Although the detailed mechanism of the above-mentioned anti-inflammatory effects of H_2 insufflation was not elucidated in the present study, this treatment may potentially serve as a novel clinical intervention in reducing the CPB-induced systemic inflammation.

CONCLUSIONS

This study demonstrated that systemic inflammatory response and organ damage including pulmonary edema were induced in the rat CPB model and that H_2 insufflation provided anti-inflammatory and organ-protective effects. We propose that H_2 insufflation could be a potential clinical therapy for counteracting CPB-induced systemic inflammation and organ damage. We consider that this rat CPB model is equivalent to already established human CPB and is useful for studying the mechanism of pathophysiological changes during artificial perfusion.

REFERENCES

1. Tatsumi E. Artificial lungs: current state and trends of clinical use and research and development. *J Artif Organs* 2007;10:1–5.
2. Walker G, Liddell M, Davis C. Extracorporeal life support-state of the art. *Paediatr Respir Rev* 2003;4:147–52.
3. Grover FL. The Society of Thoracic Surgeons National Database: current status and future directions. *Ann Thorac Surg* 1999;68:367–73.
4. Gao D, Grunwald GK, Rumsfeld JS, et al. Variation in mortality risk factors with time after coronary artery bypass graft operation. *Ann Thorac Surg* 2003;75:74–81.
5. Laffey JG, Boylan JF, Cheng DC. The systemic inflammatory response to cardiac surgery: implications for the anesthesiologist. *Anesthesiology* 2002;97:215–52.
6. Butler J, Rocker GM, Westaby S. Inflammatory response to cardiopulmonary bypass. *Ann Thorac Surg* 1993;55:552–9.
7. Schlensak C, Doenst T, Preusser S, Wunderlich M, Kleinschmidt M, Beyersdorf F. Cardiopulmonary bypass reduction of bronchial blood flow: a potential mechanism for lung injury in a neonatal pig model. *J Thorac Cardiovasc Surg* 2002;123:1199–205.
8. Hill GE, Snider S, Galbraith TA, Forst S, Robbins RA. Glucocorticoid reduction of bronchial epithelial inflammation during cardiopulmonary bypass. *Am J Respir Crit Care Med* 1995;152:1791–5.
9. Engelman RM, Rousou JA, Flack JE 3rd, Deaton DW, Kalfin R, Das DK. Influence of steroids on complement and cytokine generation after cardiopulmonary bypass. *Ann Thorac Surg* 1995;60:801–4.
10. Cremer J, Martin M, Redl H, et al. Systemic inflammatory response syndrome after cardiac operations. *Ann Thorac Surg* 1996;61:1714–20.
11. Khabar KS, Barbary MA, Khouqeer F, Devol E, al-Gain S, al-Halees Z. Circulating endotoxin and cytokines after cardiopulmonary bypass: differential correlation with duration of bypass and systemic inflammatory response/multiple organ dysfunction syndromes. *Clin Immunol Immunopathol* 1997;103:97–103.
12. Brix-Christensen V, Petersen TK, Ravn HB, Hjortdal VE, Andersen NT, Tønnesen E. Cardiopulmonary bypass elicits a pro- and anti-inflammatory cytokine response and impaired neutrophil chemotaxis in neonatal pigs. *Acta Anaesthesiol Scand* 2001;45:407–13.
13. Nakao A, Lee S, Huang C-S, Wang Z, Shigemura N, Toyoda Y. Adding a hydrogen-producing magnesium stick to the drinking water protects cardiac allografts and reduces allograft vasculopathy in rats. *J Heart Lung Transplant* 2010;29:160.
14. Hayashida K, Sano M, Ohsawa I, et al. Inhalation of hydrogen gas reduces infarct size in the rat model of myocardial ischemia-reperfusion injury. *Biochem Biophys Res Commun* 2008;373:30–5.
15. Ohsawa I, Ishikawa M, Takahashi K, et al. Hydrogen acts as a therapeutic antioxidant by selectively reducing cytotoxic oxygen radicals. *Nat Med* 2007;13:673–4.
16. Pasquale MD, Cipolle MD, Monaco J, Simon N. Early inflammatory response correlates with the severity of injury. *Crit Care Med* 1996;24:1238–42.
17. Jiang H, Meng F, Li W, Tong L, Qiao H, Sun X. Splenectomy ameliorates acute multiple organ damage induced by liver warm ischemia reperfusion in rats. *Surgery* 2007;141:32–40.
18. Boyle EM, Pohlman TH, Johnson MC, Verrier ED. Endothelial cell injury in cardiovascular surgery: the systemic inflammatory response. *Ann Thorac Surg* 1997;63:277–84.
19. Takahashi Y, Shibata T, Sasaki Y, et al. Impact of non-di-(2-ethylhexyl)phthalate cardiopulmonary bypass tubes on inflammatory cytokines and coagulation-fibrinolysis systems during cardiopulmonary bypass. *J Artif Organs* 2009;12:226–31.
20. Sebastien A, Pierre S, Claudia K, et al. Increase in levels of BDNF is associated with inflammation and oxidative stress during cardiopulmonary bypass. *Int J Biomed Sci* 2008;4:204–11.

21. Goudeau JJ, Clermont G, Guillery O, et al. In high-risk patients, combination of antiinflammatory procedures during cardiopulmonary bypass can reduce incidences of inflammation and oxidative stress. *J Cardiovasc Pharmacol* 2007;49:39–45.
22. Clermont G, Vergely C, Jazayeri S, et al. Systemic free radical activation is a major event involved in myocardial oxidative stress related to cardiopulmonary bypass. *Anesthesiology* 2002;96:80–7.
23. Ohta S. Recent progress toward hydrogen medicine: potential of molecular hydrogen for preventive and therapeutic applications. *Curr Pharm Des* 2011;17:2241–52.
24. Zhang Y, Sun Q, He B, Xiao J, Wang Z, Sun X. Anti-inflammatory effect of hydrogen-rich saline in a rat model of regional myocardial ischemia and reperfusion. *Int J Cardiol* 2011;148:91–5.
25. Lee PJ, Choi AM. Pathways of cell signaling in hyperoxia. *Free Radic Biol Med* 2003;35:341–50.
26. Koller T Jr, Hawrylenko A. Contribution to the in vitro testing of pumps for extracorporeal circulation. *J Thorac Cardiovasc Surg* 1976;54:22–9.
27. Hamamoto M, Suga M, Nakatani T, et al. Phosphodiesterase type 4 inhibitor prevents acute lung injury induced by cardiopulmonary bypass in a rat model. *Eur J Cardiothorac Surg* 2004;25:833–8.
28. Aebert H, Kirchner S, Keyser A, et al. Endothelial apoptosis is induced by serum of patients after cardiopulmonary bypass. *Eur J Cardiothorac Surg* 2000;18:589–93.

Hyperoxic Condition Promotes an Inflammatory Response During Cardiopulmonary Bypass in a Rat Model

*§Yutaka Fujii, *Mikiyasu Shirai, *Hirotsugu Tsuchimochi, ¶James T. Pearson, †Yoshiaki Takewa, †Eisuke Tatsumi, and ‡§Yoshiyuki Taenaka

*Departments of *Cardiac Physiology and †Artificial Organs; ‡Research and Development Initiative Center, National Cerebral and Cardiovascular Center Research Institute; §Graduate School of Medicine, Osaka University, Suita, Japan; and ¶Department of Physiology, and Monash Biomedical Imaging Facility, Monash University, Melbourne, Victoria, Australia*

Abstract: Systemic inflammatory responses in patients receiving cardiac surgery supported by cardiopulmonary bypass (CPB) significantly contribute to CPB-associated morbidity and mortality. We hypothesized that hyperoxia insufflation aggravates the inflammatory responses and organ damage during CPB. To verify this hypothesis, we investigated the inflammatory responses at high and normal levels of arterial pressure of oxygen (PaO_2) in the rat CPB model. Rats were divided into a SHAM group, a hyperoxia CPB group ($PaO_2 > 400$ mm Hg), and a normoxia CPB group (PaO_2: 100–150 mm Hg). We measured the serum cytokine levels of tumor necrosis factor-α, interleukin (IL)-6, and IL-10, and biochemical markers (lactate dehydrogenase, aspartate aminotransferase, and alanine aminotransferase) before, 60, and 120 min after the initiation of CPB. We also measured the wet-to-dry weight (W/D) ratio of the left lung and performed dihydroethidium (DHE) stain reflecting superoxide generation in the lung and liver tissues 120 min after the CPB initiation. In the hyperoxia group, the pro-inflammatory cytokines and biochemical markers significantly increased during the CPB compared with the SHAM, but such increases were significantly suppressed in the normoxia group. However, the increase in anti-inflammatory cytokines was more suppressed in the hyperoxia group than in the normoxia group. The W/D ratio increased significantly more in the hyperoxia group than in the normoxia group. In addition, the DHE fluorescence predominantly increased in the hyperoxia group compared with that in the normoxia group. These data suggest that it is better to avoid too much oxygen insufflation for attenuating organ damage associated with the superoxide production and inflammatory responses during CPB.
Key Words: Cardiopulmonary bypass model—Systemic inflammation—Hyperoxia—Superoxide—Cytokine.

Extracorporeal life support devices, such as cardiopulmonary bypass (CPB), preserve the patient's life by providing adequate oxygen supply and blood flow to vital organs (1). However, cardiac surgery with the use of CPB is often accompanied by a systemic inflammatory response, significantly influencing the morbidity and mortality after CPB (2).

Possible factors responsible for the inflammatory response are blood contact with the surface of the extracorporeal circulation unit, endotoxemia, surgical trauma, ischemic reperfusion injury, and blood loss (3). The increase in cytokines, such as interleukins (ILs), necrosis factor, and bradykinin (4), aggravates the inflammatory response during CPB (5). Our recent study has shown that CPB causes a systemic inflammatory response and organ damage in the rat CPB model (6).

In addition, a recent study has shown that among patients admitted to the intensive care units following resuscitation from cardiac arrest, the hyperoxia management group had significantly higher in-hospital mortality compared with the normoxia

doi:10.1111/aor.12125

Received February 2013; revised April 2013.
Address correspondence and reprint requests to Mr. Yutaka Fujii, Department of Cardiac Physiology, National Cerebral and Cardiovascular Center Research Institute, 5-7-1 Fujishiro-dai, Suita 565-8565, Japan. E-mail: yfujii@ri.ncvc.go.jp; yyyyyfujii@gmail.com

management group (7). Lee and Choi (8) previously showed that hyperoxia induces oxidative cell damage by promoting the formation of reactive oxygen species (ROS) and the expression of inflammatory cytokines (8). Currently, however, arterial pressure of oxygen (PaO_2) is maintained at very high levels in clinical CPB (9).

We hypothesized that too much oxygen aggravates the systemic inflammatory response and causes organ tissue damage during CPB. We considered that appropriate control of oxygen would attenuate the systemic inflammatory response with a reduction of inflammatory cytokine levels, providing protective effects against organ tissue damage during CPB. To verify this hypothesis, we investigated the effect of high and normal PaO_2 on the levels of serum cytokines: tumor necrosis factor-α (TNF-α), IL-6, and IL-10, and biochemical markers: lactate dehydrogenase (LDH), aspartate aminotransferase (AST), and alanine aminotransferase (ALT) in a rat CPB model. In addition, we measured the lung wet-to-dry weight (W/D) ratio as an index of pulmonary edema. Moreover, we performed dihydroethidium (DHE) staining for detecting superoxide production in the lung and liver tissues.

MATERIALS AND METHODS

Animal

The study was approved by the National Cerebral and Cardiovascular Center Research Institute Animal Care and Use Committee, and all procedures met the National Institutes of Health guidelines for animal care.

Sprague-Dawley rats (male 400–450 g) were housed three per cage under a 12-h light-dark cycle with food and water available ad libitum.

Anesthesia, surgical preparation, and CPB

The animals were anesthetized with pentobarbital sodium (50 mg/kg body weight, intraperitoneal injection) and placed in the supine position with rectal thermocouple in place. Then, orotracheal intubation was performed using a 14G cannula (Insyte BD Medical, Sandy, UT, USA) and rats were ventilated with a respirator (Model SN-480-7, Shinano Seisakusho Co., Ltd, Tokyo, Japan). Ventilation was volume controlled at a frequency of 70/min, a tidal volume of 8–10 mL/kg body weight, and 40% of inspired oxygen fraction. Rectal temperature was maintained at 36°C throughout the experiment. Arterial blood pressure was monitored (Model 870, PowerLab system, AD Instruments, Castle Hill, NSW, Australia) via the femoral artery, which was cannulated with polyethylene tubing (SP-31 Natsume Seisakusho Co., Ltd, Tokyo, Japan). The left common carotid artery was cannulated with a polyethylene tubing (SP-55 Natsume Seisakusho Co.) to serve as the arterial inflow cannula for the CPB circuit. Heparin sodium (500 IU/kg) was administered after placement of this cannula. A 16G cannula (Insyte BD Medical) was advanced through the right external jugular vein into the right atrium and served as a conduit for venous outflow.

The CPB circuit consisted of a membranous oxygenator (Senko Medical Co., Ltd, Osaka, Japan), tubing line (Senko Medical Co., Ltd), and roller pump (Micro tube pump MP-3, Tokyo Rikakikai Co., Ltd, Tokyo, Japan) primed by 8 mL of Ringer's solution, 3 mL of mannitol, 3 mL of sodium bicarbonate, and 1 mL (1000 IU) of heparin.

Experimental design

The animals were divided into three groups: SHAM group ($n = 5$), hyperoxia CPB group ($n = 7$), and normoxia CPB group ($n = 7$). The SHAM group received surgical preparation only without CPB and PaO_2 was maintained at 100–150 mm Hg during the experiment. In the hyperoxia CPB group, PaO_2 during CPB was maintained at greater than 400 mm Hg. In the normoxia CPB group, PaO_2 during CPB was maintained at 100–150 mm Hg. In all experiments, CPB pump flow was maintained at 70 mL/kg/min. In all groups, arterial pressure of carbon dioxide ($PaCO_2$) was maintained at 35–45 mm Hg.

Blood samples were collected at three defined time points, before CPB (pre-CPB), 60 min after initiation of CPB, and 120 min after initiation of CPB (end-CPB).

To evaluate the inflammatory responses (10), TNF-α, IL-6, and IL-10 were measured by enzyme-linked immunosorbent assay (Quantikine ELISA kit, R&D Systems, Minneapolis, MN, USA). The concentrations of LDH, AST, and ALT were used as biochemical markers for evaluating organ damage (11) and were measured by automated colorimetry from blood plasma samples (DRI-CHEM 7000 Analyzer, FUJIFILM, Kanagawa, Japan).

Blood gases, pH, hemoglobin (Hb) concentration, and electrolytes were also measured (ABL800 FLEX system, RADIOMETER, Copenhagen, Denmark). Animals in which the Hb level declined to less than 7 g/dL at any point were excluded from the study. All animals were sacrificed at the end of CPB by potassium chloride injection into the heart and the left lung was harvested and divided into three parts. The superior third was used for the calculation of W/D

ratio. The lung block was weighed before and after desiccation for 72 h in a dry oven at 70°C. Additionally, the right lung and a part of the liver were placed in cold phosphate-buffered saline and then embedded using the dry ice acetone method for cryosectioning. The frozen segments were cut into 7-μm-thick transverse sections that were then placed on glass slides. DHE stain solution (Wako Pure Chemical Industries, Ltd, Osaka, Japan) diluted with dimethyl sulfoxide 30 000 times was topically applied to each tissue section. The slides were incubated in a light-protected chamber at 37°C for 30 min. Images of the tissue sections were obtained using a fluorescence microscope (red fluorescence, 594 nm) (Olympus Corporation, Tokyo, Japan) with a rhodamine filter. Fluorescence intensity, which positively correlates with the amount of surperoxide generation, was determined in the lung and liver tissue using Image J software (NIH, Bethesda, MD, USA).

Statistics

All data are expressed as mean ± standard error. Comparison among groups was performed using analysis of variance. Fisher's protected least significant difference post hoc test was used for subsequent comparison between groups at the same time points. All statistical analyses were performed using StatView 5.0 (Abacus Concepts, Berkeley, CA, USA). Significance was set at $P < 0.05$.

RESULTS

Table 1 shows the changes in hemodynamic variables, Hb concentration, and PaO_2 and $PaCO_2$ in SHAM, hyperoxia CPB, and normoxia CPB groups during experiments. Mean arterial pressure (MAP) and Hb were significantly decreased during CPB in both hyperoxia and normoxia CPB groups. However, there were no statistical differences in such decreases between these groups. The PaO_2 level was much higher in the hyperoxia CPB group (~460 mm Hg) than in the normoxia CPB group (~130 mm Hg), while no statistical difference was found in the $PaCO_2$ level between these groups.

Before CPB, the serum levels of inflammatory and biochemical markers were not statistically different among the SHAM, hyperoxia CPB, and normoxia CPB groups. Serum inflammatory and biochemical markers remained unchanged during experiment periods in the SHAM group. In the hyperoxia CPB group, the pro-inflammatory cytokines increased significantly, reaching a maximum (TNF-α: 1237 ± 62 pg/mL, IL-6: 1695 ± 73 pg/mL) at the end of CPB. In the normoxia CPB group, however, the increases in the pro-inflammatory cytokines were significantly suppressed by 38~40% compared with the hyperoxia CPB group (Fig. 1a,b). In contrast, in the normoxia CPB group, the anti-inflammatory cytokine increased significantly, reaching a maximum (IL-10: 1003 ± 36 pg/mL) at the end of CPB, 62% higher in comparison with the hyperoxia CPB group at the same time point (Fig. 1c).

In the hyperoxia CPB group, the levels of biochemical markers significantly increased (LDH: 447 ± 48 U/L, AST: 143 ± 12 U/L, ALT: 46 ± 7 U/L) 60 min after the CPB initiation and increased further (LDH: 882 ± 62 U/L, AST: 233 ± 20 U/L, ALT: 92 ± 11 U/L) 120 min after the CPB initiation. In the

TABLE 1. *Hemodynamic variables, Hb, and blood gas partial pressures before and during CPB*

	Group	Pre-CPB	CPB 60 min	CPB 120 min
MAP (mm Hg)	SHAM	103 ± 3	100 ± 5	104 ± 3
	Hyperoxia CPB	105 ± 5	80 ± 3†	76 ± 3†
	Normoxia CPB	104 ± 5	87 ± 3	80 ± 3†
HR (beats/min)	SHAM	385 ± 15	385 ± 11	381 ± 7
	Hyperoxia CPB	406 ± 9	358 ± 8	363 ± 8
	Normoxia CPB	401 ± 5	373 ± 3	364 ± 4
PaO_2 (mm Hg)	SHAM	113 ± 8	106 ± 7	105 ± 6
	Hyperoxia CPB	103 ± 8	464 ± 17†*	461 ± 16†*
	Normoxia CPB	106 ± 3	127 ± 11	137 ± 8
$PaCO_2$ (mm Hg)	SHAM	38 ± 1	37 ± 1	40 ± 1
	Hyperoxia CPB	40 ± 1	37 ± 1	36 ± 1
	Normoxia CPB	41 ± 1	40 ± 1	41 ± 1
Hb (mg/dL)	SHAM	15.3 ± 1.0	15.2 ± 0.5	14.5 ± 0.4
	Hyperoxia CPB	15.4 ± 0.2	10.1 ± 0.5†	9.8 ± 0.4†
	Normoxia CPB	15.8 ± 0.4	10.4 ± 0.6†	9.9 ± 0.4†

Variables are expressed as mean ± standard error.
† $P < 0.05$ versus SHAM group at the same time, * $P < 0.05$ versus normoxia CPB group at the same time. HR, heart rate.

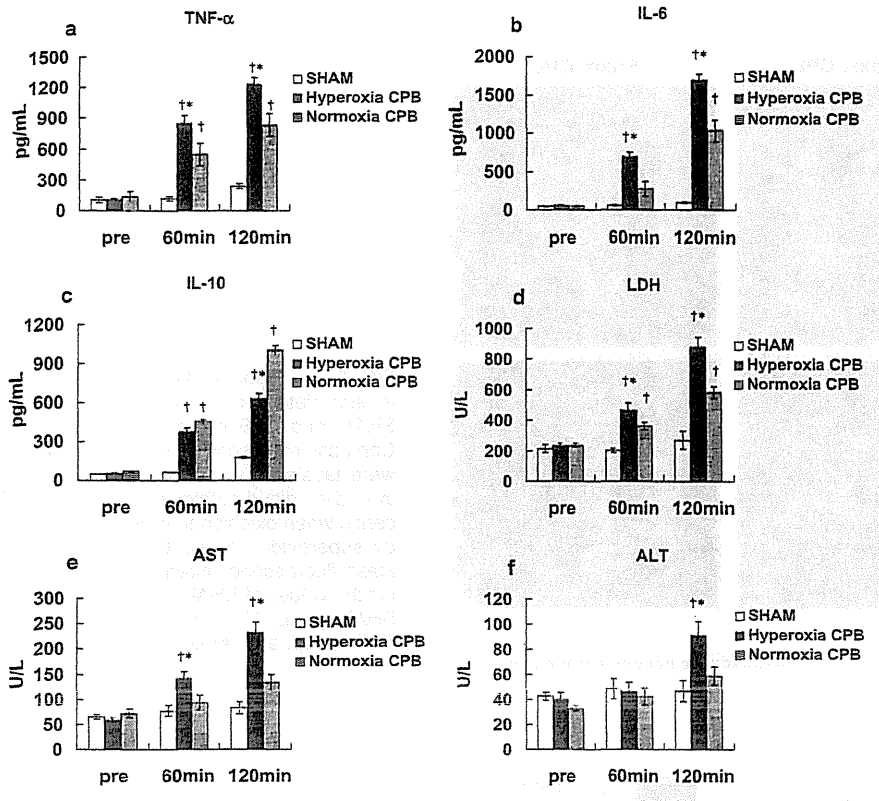

FIG. 1. Serum TNF-α (a), IL-6 (b), IL-10 (c), LDH (d), AST (e), ALT (f). †$P < 0.05$ versus SHAM group, *$P < 0.05$ versus normoxia CPB group at the same time periods.

normoxia CPB group, however, the elevated levels of biochemical markers were significantly suppressed by 47–64% 120 min after the CPB initiation as compared with the hyperoxia CPB group (Fig. 1d–f). Neither AST or ALT levels changed significantly during CPB from the pre-CPB level in the normoxia group.

The CPB groups showed significantly higher W/D ratio than the SHAM group. (SHAM: 4.68 ± 0.08, hyperoxia CPB: 6.01 ± 0.10, normoxia CPB: 5.57 ± 0.08) (Fig. 2) However, the increase in W/D ratio was significantly suppressed in the normoxia CPB group compared with the hyperoxia CPB group.

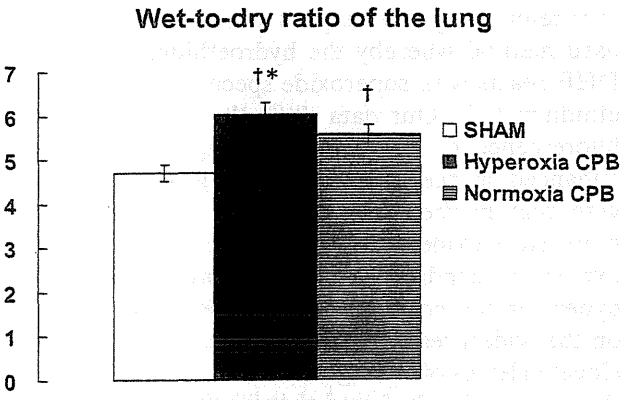

FIG. 2. Wet-to-dry ratio of the left lung at the end of CPB. †$P < 0.05$ versus SHAM group, *$P < 0.05$ versus normoxia CPB group.

DHE staining in the lung and liver tissues was markedly enhanced in the hyperoxia CPB group compared with that in the normoxia CPB group (Fig. 3a,b), indicating greater superoxide production with an increased oxygen supply.

DISCUSSION

We demonstrated for the first time that the pro-inflammatory cytokines and biochemical markers for organ damages increased significantly more in the hyperoxia group than those in the normoxia group during CPB in the rat. At the same time, the increase in an anti-inflammatory cytokine was more suppressed in the hyperoxia group than in the normoxia group. The lungs of rats in the hyperoxia group had higher W/D ratio at the end of CPB than the normoxia group and therefore are presumed to have accumulated more water. In addition, the DHE staining for superoxide production indicated that there was a marked increase in the lung and liver tissues in the hyperoxia group, but not in the normoxia group.

In the present study, the serum cytokine levels (TNF-α, IL-6, IL-10) and biochemical markers (LDH, AST, ALT) were significantly elevated in the CPB groups compared with the SHAM group,

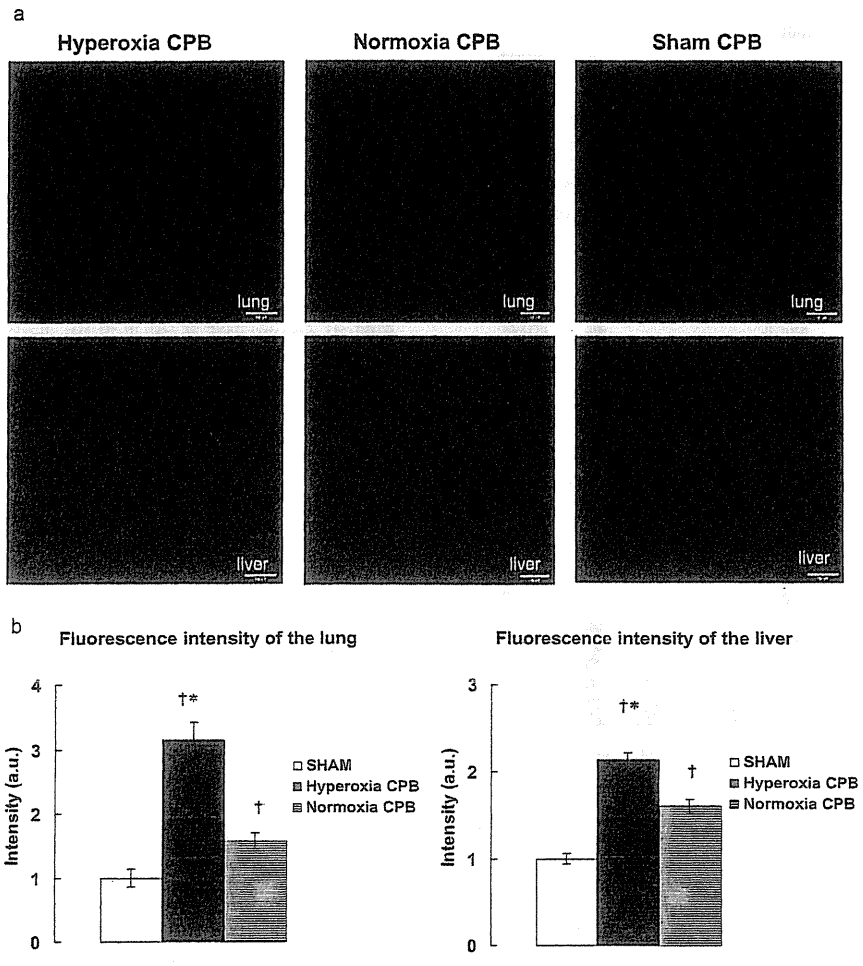

FIG. 3. (a) Representative examples of in situ detection of superoxide in the SHAM and CPB groups' lung and liver. Confocal microscope sections of organ were labeled with the fluorescent oxidative dye dihydroethidium (red fluorescence when oxidized to ethidium bromide by superoxide). Scale bar: 100 μm. (b) Mean fluorescence intensity after deducting the values of SHAM. †$P < 0.05$ versus SHAM group, *$P < 0.05$ versus normoxia CPB group. a.u.: arbitrary unit.

indicating that a systemic inflammatory response and organ damage occurred in our rat CPB model. However, systemic blood pressure and Hb were maintained around 80 mm Hg and 10 g/dL, respectively, during the CPB. From these data, our rat CPB model is considered to be equivalent to the established human CPB procedure, which is often associated with systemic inflammation and organ damage (12).

Possible factors responsible for the inflammatory response during CPB are blood contact with the surface of the extracorporeal circulation unit, endotoxemia, surgical trauma, ischemic reperfusion injury, and blood loss (3). Many studies have shown that the walls of the CPB circuit activate white cells, platelets, and the complement system. Activated leukocytes release cytotoxic agents and ROS associated with systemic inflammation and organ damage (13,14). The increase in cytokines, such as ILs and necrosis factor (4), aggravates the inflammatory response (5). Thus, these complex interactions during CPB lead to further inflammation (5).

We hypothesized that abnormally elevated oxygen levels stimulate production of ROS and aggravate the systemic inflammatory response and organ tissue damage during CPB. The primary product in cellular ROS production is the superoxide anion. In this study, DHE stain fluorescence was used for detecting intracellular superoxide production. This is a widely used method whereby the hydroethidine moiety of DHE reacts with superoxide specifically to produce ethidium (15). Our data show that the DHE stain fluorescence of the liver and lung was markedly enhanced in the hyperoxia CPB group compared with that in the normoxia CPB group, indicating more superoxide production during CPB with the hyperoxic condition. We therefore suggest that hyperoxia caused direct oxidative cell damage based on the widespread increase in ROS production and elevated levels of damage markers (16). In relation to this, we previously found that insufflation of hydrogen gas suppressed the increase in the organ damage markers during CPB in the rat by removing the hydroxyl radical (the most cytotoxic radical) (12).

Because ROS activates T-lymphocytes and cytokine production via redox-sensitive signal pathways (17), it is also possible that hyperoxia increased the cytokine expression via elevated ROS production in our rat CPB model. Our data showed that the pro-inflammatory markers (TNF-α, IL-6) and biochemical makers for organ damages (LDH, AST, ALT) were significantly elevated in the hyperoxia CPB group compared with the normoxia CPB and SHAM groups. This study demonstrated that not only did hyperoxia significantly increase serum pro-inflammatory cytokines and organ damage during CPB, but it also significantly suppressed expression of the anti-inflammatory cytokine (IL-10) compared with the normoxia group. This suppression is considered to have enhanced the inflammatory responses in the hyperoxia CPB group, as IL-10 is an anti-inflammatory cytokine that regulates the production of pro-inflammatory cytokines (18). Our findings therefore indicate that appropriate oxygen control not only attenuates pro-inflammatory cytokine generation, but also increases anti-inflammatory cytokine generation, reducing the inflammatory responses during CPB in the rat.

Our previous study showed that the selective reduction of hydroxyl radical with hydrogen gas attenuates both pro- and anti-inflammatory cytokines, suggesting that this radical acts to nonselectively increase these cytokines (6). The mechanism for the present finding whereby hyperoxia increases pro-inflammatory cytokines, but decreases anti-inflammatory cytokines under the condition of increased superoxide production, is not clear. It is possible that hyperoxia influences cytokine responses through a mechanism other than the ROS pathway. It should be noted, however, that there is a report that hyperoxia downregulated the anti-inflammatory cytokine IL-10 gene in fetal rat alveolar type II cells in cell culture at least (19).

The increased W/D ratio of the lung reported here suggests that pulmonary edema occurred during CPB. This is consistent with an earlier clinical study (20) and our previous rat CPB model study (6). A new finding in the present study is that this increase in the W/D ratio was attenuated by reducing the extent of oxygen oversupply during CPB. Because the earliest signs of hyperoxic lung cell injury are found in pulmonary capillary endothelial cells in hyperoxic lungs (21,22), it is possible that maintenance of normoxic conditions attenuates the injury of the vascular endothelium by suppressing the production of superoxide and pro-inflammatory cytokines during CPB. Of note, there is one human study that reports that hyperoxic exposure for an average of 17 h is not associated with a significant influx of neutrophils to the alveolar structures, but causes alterations in alveolar capillary permeability with alveolar macrophages secreting mediators (23).

Limitations

This study has several limitations. First, we suggested that hyperoxic CPB aggravates the inflammatory response and tissue injury from the changes in the levels of serum cytokines and biochemical markers. However, histological evaluation of tissue inflammation was limited to the lung and liver. Further studies of other organs, especially vital organs such as heart and brain, are needed to verify this suggestion. Second, we maintained PaO_2 at 100–150 mm Hg and greater than 400 mm Hg in the normoxic and hyperoxic CPB, respectively. Further studies are needed to focus on PaO_2 ranging from 200 to 300 mm Hg, which is more applicable in clinical practice. Finally, we consider that our rat model of CPB is equivalent to the established human CPB procedure. However, it is necessary to study the effect of PaO_2 level on the inflammatory responses during CPB in larger animal models before we can consider applying our findings to clinical practice.

CONCLUSIONS

This study showed that the systemic inflammatory response and organ damage including pulmonary edema were induced associated with the production of cytokines and superoxide in the rat cardiopulmonary bypass model. The hyperoxic condition aggravated these responses while enhancing and attenuating the productions of pro-inflammatory and anti-inflammatory cytokines, respectively. We suggest that it is better to maintain appropriate oxygen concentrations (not hyperoxic) to minimize probability of the systemic inflammatory response and organ damage during CPB, although normoxic CPB does not completely eliminate these responses. Additionally, we suggest that this rat CPB model might be equivalent to the established human CPB procedure and useful for studying the mechanism of pathophysiological changes during artificial perfusion.

REFERENCES

1. Walker G, Liddell M, Davis C. Extracorporeal life support-state of the art. *Paediatr Respir Rev* 2003;4:147–52.
2. Gao D, Grunwald GK, Rumsfeld JS, et al. Variation in mortality risk factors with time after coronary artery bypass graft operation. *Ann Thorac Surg* 2003;75:74–81.
3. Butler J, Rocker GM, Westaby S. Inflammatory response to cardiopulmonary bypass. *Ann Thorac Surg* 1993;55:552–9.

4. Engelman RM, Rousou JA, Flack JE 3rd, Deaton DW, Kalfin R, Das DK. Influence of steroids on complement and cytokine generation after cardiopulmonary bypass. *Ann Thorac Surg* 1995;60:801–4.
5. Cremer J, Martin M, Redl H, et al. Systemic inflammatory response syndrome after cardiac operations. *Ann Thorac Surg* 1996;61:1714–20.
6. Fujii Y, Shirai M, Inamori S, et al. Insufflation of hydrogen gas restrains the inflammatory response of cardiopulmonary bypass in a rat model. *Artif Organs* 2013;37:136–41.
7. Kilgannon JH, Jones AE, Shapiro NI, et al.; Emergency Medicine Shock Research Network (EMShockNet) Investigators. Association between arterial hyperoxia following resuscitation from cardiac arrest and in-hospital mortality. *JAMA* 2010;303:2165–71.
8. Lee PJ, Choi AM. Pathways of cell signaling in hyperoxia. *Free Radic Biol Med* 2003;35:341–50.
9. Morita K. Surgical reoxygenation injury of the myocardium in cyanotic patients: clinical relevance and therapeutic strategies by normoxic management during cardiopulmonary bypass. *Gen Thorac Cardiovasc Surg* 2012;60:549–56.
10. Pasquale MD, Cipolle MD, Monaco J, Simon N. Early inflammatory response correlates with the severity of injury. *Crit Care Med* 1996;24:1238–42.
11. Jiang H, Meng F, Li W, Tong L, Qiao H, Sun X. Splenectomy ameliorates acute multiple organ damage induced by liver warm ischemia reperfusion in rats. *Surgery* 2007;141:32–40.
12. Boyle EM, Pohlman TH, Johnson MC, Verrier ED. Endothelial cell injury in cardiovascular surgery: the systemic inflammatory response. *Ann Thorac Surg* 1997;63:277–84.
13. Goudeau JJ, Clermont G, Guillery O, et al. In high-risk patients, combination of antiinflammatory procedures during cardiopulmonary bypass can reduce incidences of inflammation and oxidative stress. *J Cardiovasc Pharmacol* 2007;49:39–45.
14. Clermont G, Vergely C, Jazayeri S, et al. Systemic free radical activation is a major event involved in myocardial oxidative stress related to cardiopulmonary bypass. *Anesthesiology* 2002;96:80–7.
15. Jones CI 3rd, Han Z, Presley T, et al. Endothelial cell respiration is affected by the oxygen tension during shear exposure: role of mitochondrial peroxynitrite. *Am J Physiol Cell Physiol* 2008;295:180–91.
16. Pagano A, Barazzone-Argiroffo C. Alveolar cell death in hyperoxia-induced lung injury. *Ann N Y Acad Sci* 2003;1010:405–16.
17. Dröge W. Free radicals in the physiological control of cell function. *Physiol Rev* 2002;82:47–95.
18. Opal SM, DePalo VA. Anti-inflammatory cytokines. *Chest* 2000;117:1162–72.
19. Lee HS, Kim CK. Effect of recombinant IL-10 on cultured fetal rat alveolar type II cells exposed to 65%-hyperoxia. *Respir Res* 2011;12:68.
20. Aebert H, Kirchner S, Keyser A, et al. Endothelial apoptosis is induced by serum of patients after cardiopulmonary bypass. *Eur J Cardiothorac Surg* 2000;18:589–93.
21. Kistler GS, Caldwell PR, Weibel ER. Development of fine structural damage to alveolar and capillary lining cells in oxygen-poisoned rat lungs. *J Cell Biol* 1967;32:605–28.
22. Zaher TE, Miller EJ, Morrow DM, Javdan M, Mantell LL. Hyperoxia-induced signal transduction pathways in pulmonary epithelial cells. *Free Radic Biol Med* 2007;42:897–908.
23. Davis WB, Rennard SI, Bitterman PB, Crystal RG. Pulmonary oxygen toxicity. Early reversible changes in human alveolar structures induced by hyperoxia. *N Engl J Med* 1983;309:878–83.

Society For Biomaterials

Preparation of an autologous heart valve with a stent (stent-biovalve) using the stent eversion method

Takeshi Mizuno,[1,2] Yoshiaki Takewa,[3] Hirohito Sumikura,[3] Kentaro Ohnuma,[3] Takeshi Moriwaki,[1] Masashi Yamanami,[1] Tomonori Oie,[1] Eisuke Tatsumi,[3] Masami Uechi,[1,2] Yasuhide Nakayama[1]

[1]Division of Medical Engineering and Materials, National Cerebral and Cardiovascular Center Research Institute, Osaka, Japan

[2]Department of Veterinary Medicine, Veterinary Cardiovascular Medicine and Surgery Unit, Laboratory of Veterinary Internal Medicine, College of Bioresource Sciences, Nihon University, Kanagawa, Japan

[3]Department of Artificial Organs, National Cerebral and Cardiovascular Center Research Institute, Osaka, Japan

Received 26 October 2013; accepted 19 November 2013
Published online 00 Month 2013 in Wiley Online Library (wileyonlinelibrary.com). DOI: 10.1002/jbm.b.33086

Abstract: We designed a novel method for constructing an autologous heart valve with a stent, called a stent-biovalve. In constructing completely autologous heart valves, named biovalves, which used in-body tissue architecture technology, tissues for leaflets were formed via ingrowths into narrow apertures in the preparation molds, frequently leading to delayed or incomplete biovalve preparation. In this technique, self-expandable nitinol stents after everting were mounted on an acrylic column-shaped part and partially covered with an acrylic cylinder-shaped part with three slits. This assembled mold was placed into subcutaneous abdominal pouches in beagles or goats for 4 weeks. Upon removing the acrylic parts after harvesting and trimming of capsulated tissues, a tubular hollow structure with three pocket-flaps of membranous tissue rigidly fixed to the stent's outer surface was obtained. Then, the stent was turned inside out to the original form, thus moving the pocket-flaps from outside to the inside. Stent-biovalves with a sufficient coaptation area were thus obtained with little tissue damage in all cases. The valve opened smoothly, and high aperture ratio was noted. This novel technique was thus highly effective in constructing a robust, completely autologous stent-biovalve with adequate valve function. © 2013 Wiley Periodicals, Inc. J Biomed Mater Res Part B: Appl Biomater 00B: 000–000, 2013.

Key Words: heart valve, autologous tissue, stent, biovalve

How to cite this article: Mizuno T, Takewa Y, Sumikura H, Ohnuma K, Moriwaki T, Yamanami M, Oie T, Tatsumi E, Uechi M, Nakayama Y. 2013. Preparation of an autologous heart valve with a stent (stent-biovalve) using the stent eversion method. J Biomed Mater Res Part B 2013: 00B: 000–000.

INTRODUCTION

Aortic valve disease is one of the most major heart diseases in humans. Once symptoms develop, the average survival of patients with aortic stenosis is reduced to <5 years.[1–3] Patients with severe valvular insufficiency or stenosis typically require valve repair or valve replacement. Surgery for end-stage valvular heart disease consists of two basic alternatives, mechanical and biological prostheses, both of which have significant limitations.[4] While mechanical valves have a functional life span of at least 25 years, they are associated with the need for life-long anticoagulation treatment and the concomitant risks of thromboembolism and bleeding. Biological prostheses generally have better hemodynamic characteristics and do not require long-term aniticoagulation therapies, but are associated with progressive tissue deterioration. Since surgical valve replacement is a highly invasive surgery involving thoracotomy and cardiopulmonary bypass, elderly patients and those with extensive comorbidities cannot undergo this surgery. Since 2002,[5] the less invasive transcatheter aortic valve implantation (TAVI) has been introduced for inoperable and high-risk patients. Recently, with technological advancements, the clinical application of TAVI has extended to intermediate-risk patients.[6] TAVI is expected to evolve further and become more commonly used in the future. However, using a bioprosthetic valve for TAVI has certain disadvantages, since it undergoes progressive degeneration and calcification as it contains no living cells.[7,8]

To overcome these limitations, living heart valves—created by tissue engineering—have been under development. Some heart valves created by tissue engineering have been successfully implanted in animals.[9,10] However, these valves require complicated cell management protocols with cell culture in bioreactors under strictly sterile conditions; this procedure is time-consuming and expensive.

We have previously developed autologous prosthetic tissues by using the "in-body tissue architecture (IBTA)" technology, which is a novel and practical approach for regenerative medicine based on the tissue encapsulation phenomenon of foreign materials in living bodies.[11] This

Correspondence to: Y. Nakayama (e-mail: ny@ncvc.go.jp)

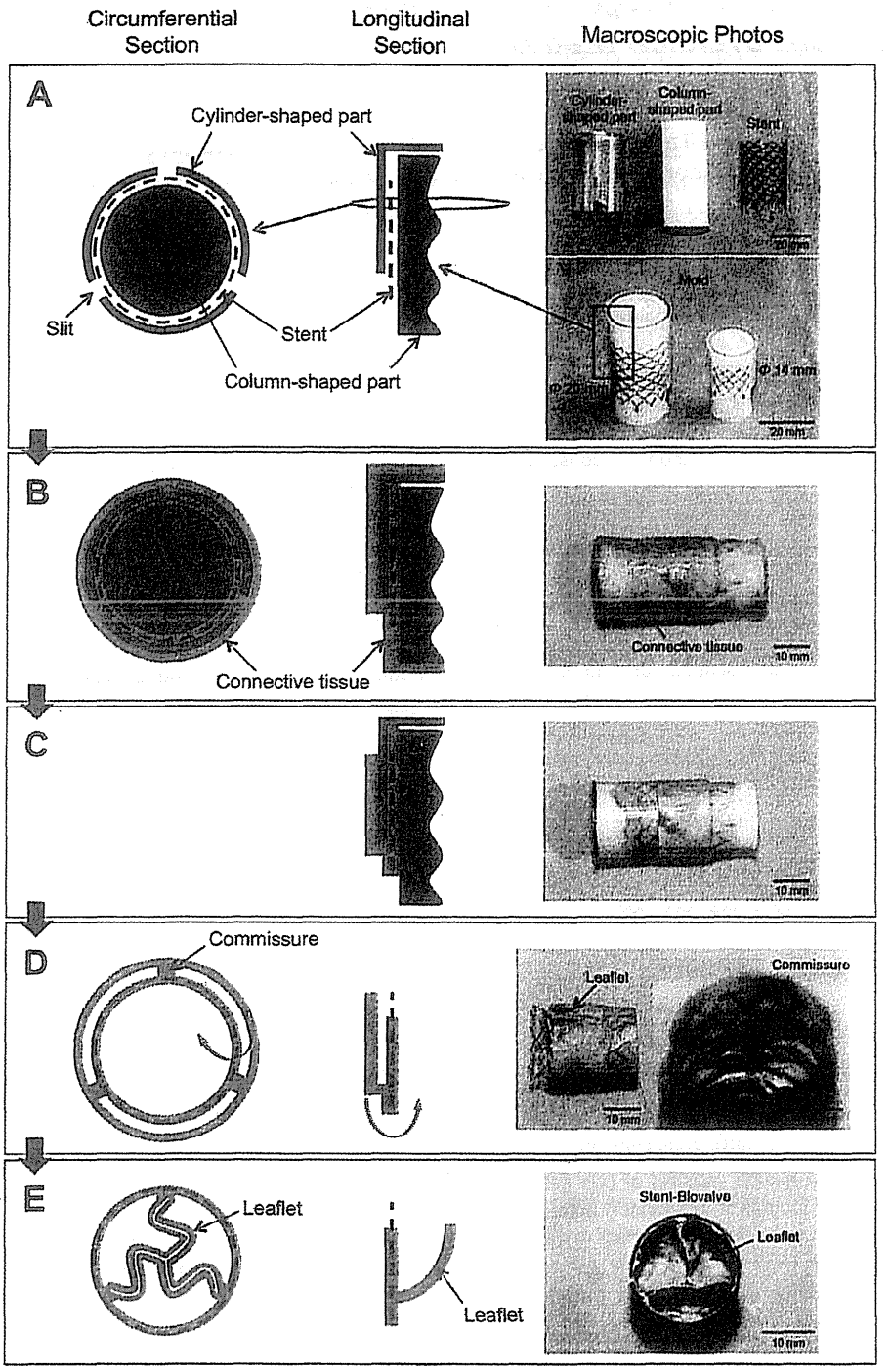

technology involves the use of living bodies as a reactor, and does not need expensive facilities or complicated manipulations. We have reported the construction of completely autologous trileaflet heart valves, named biovalves, prepared using this technology,[11–15] which may resolve the abovementioned problems encountered with

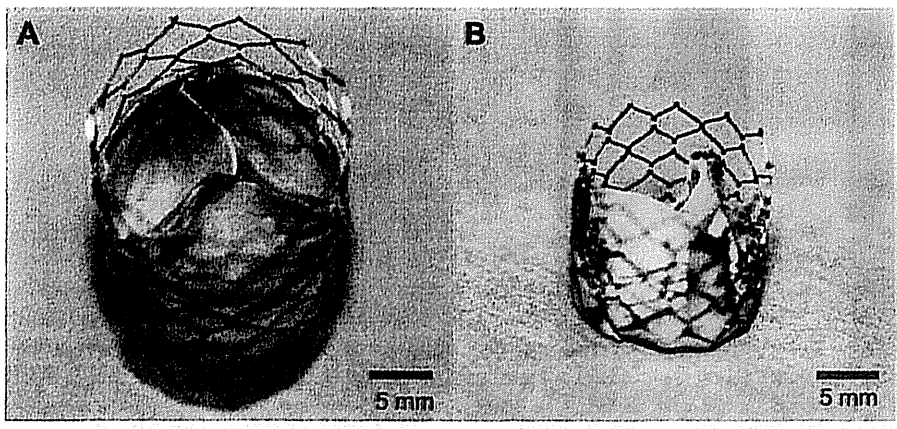

FIGURE 2. The obtained stent-biovalves with diameter of 20 mm (A) and 14 mm (B). [Color figure can be viewed in the online issue, which is available at wileyonlinelibrary.com.]

bioprosthetic valves. In fact, biovalves have been demonstrated to have excellent valve function and histological changes when implanted as a pulmonary valve in a beagle model[16] and an aortic valve in a goat model.[17] In these biovalves, leaflet formation occurs by tissue ingrowth into narrow apertures in the preparation molds from the connective tissues surrounding the molds. During the encapsulation process, the conduit portion of the biovalve is completely formed within ~4 weeks of embedding, similar to the biotubes, which are autologous vascular grafts from IBTA. However, because tissue migration into a narrow aperture is slow in general, leaflet formation in the biovalve required a longer time than that required for conduit formation.

In this study, to further improve the biovalve design and to adapt it for transcatheter valve replacement, we attempted to combine the biovalve design with a self-expandable nitinol stent to construct a "stent-biovalve." The preparation mold was designed based on a novel concept, in which the leaflet tissue was formed on the outer side of the mold; the trileaflet-shaped valve was obtained by finally everting the stent such that the leaflet tissue existed inside surface of the stent. The valvular function of the stent-biovalve was examined by using an *in vitro* circulation circuit.

MATERIALS AND METHODS

Animal studies

Studies were performed in accordance with the "Guide for the Care and Use of Laboratory Animals" published by the US National Institutes of Health (NIH Publication No. 85-23, revised 1996) under a protocol approved by the National Cerebral and Cardiovascular Center Research Institute Committee (No. 12002).

Mold assembling

Two kind of stents used were self-expandable (diameter = 14 mm; length = 15 mm or diameter = 20 mm; length = 30 mm), obtained from shape rememory of E-LUMINEXX (diameter = 12 mm; length = 100 mm; Bard, Karlsruhe, Germany) by Piolax Medical Devices (Yokohama, Japan) and cutting.

The mold for the stent-biovalve was obtained by assembling the stent, a specially designed column-shaped acrylic part (outer diameter = 14 mm; length = 32 mm for 14 mm-sized stent, and outer diameter = 20 mm; length = 46 mm for 20 mm-sized stent), and cylinder-shaped acrylic part (outer diameter = 17 mm; length = 18 mm for 14 mm-sized stent, and outer diameter = 23 mm; length = 34 mm for 20 mm-sized stent) with three slits (width = 1 mm; length = 10 mm for 14 mm-sized stent, and width = 1 mm; length = 15 mm for 20 mm-sized stent) [Figure 1(A)]. All acrylic parts were prepared using a 3D printer (CONNEX 260, Objet, Rehovot, Israel). After gently everting the stent in ice water, it was mounted on the column-shaped acrylic part and then covered with the cylinder-shaped part for the final mold.

Preparation of stent-biovalves

A beagle dog (age: 1 year; body weight: 10 kg) under general anesthesia induced by intramuscular injection of ketamine (20 mg/kg), or a goat (age: 1 year; body weight: 50 kg) under general anesthesia induced with 10 mg/kg of ketamine and maintained with 1–3% isoflurane was used for the stent-biovalve preparation. After 4 weeks of mold embedding in the abdominal subcutaneous pouches of each animal, the implants, which were completely encapsulated with connective tissue, were harvested [Figure 1(B)]. The fragile, irregular, and redundant tissues around the developed tubular tissue were gently cut, and three leaflet parts were obtained by trimming the capsulated tissue [Figure 1(C)]. The acrylic cylinder- and column-shaped parts were removed. The stent, now embedded in connective tissue, also showed three flaps of membranous connective tissue on its outer surface [Figure 1(D)]. The stent was then everted to its original form in ice water to obtain the stent-biovalve, with a tri-leaflet valve on its inner surface [Figure 1(E)]. The stent-biovalves with diameter of 20 mm [Figure 2(A)] were prepared from goats and those of 14 mm [Figure 2(B)] were from beagles.

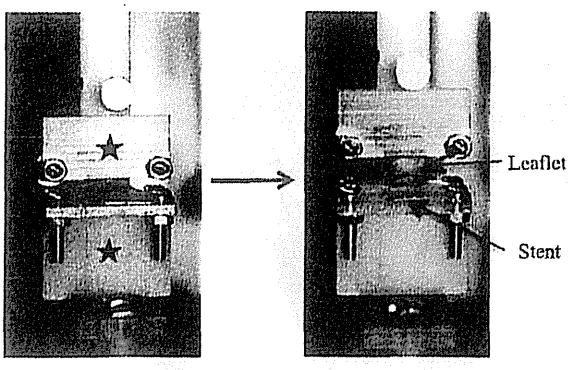

FIGURE 3. Photographs of sample folder in the apparatus for connective strength measurement before (A) and after (B) stretching. [Color figure can be viewed in the online issue, which is available at wileyonlinelibrary.com.]

Histological evaluation

The leaflets of the stent-biovalve were fixed in 10% formalin solution and embedded in paraffin. Then leaflet sections were cut into pieces 3–5 μm thick for hematoxyline and eosin staining or masson's trichrome stain. The wall thickness of the leaflets was measured by microscopic observation of the sections.

Measurement of mechanical properties

The burst strength of the leaflet tissues of stent-biovalve was determined by using a specially designed apparatus. The specimens were fixed on a sample holder with a hole (diameter = 2 mm) at its center. Saline solution was introduced into this apparatus at a rate of 50 mmHg/s. The burst strength was determined by measuring the water pressure at the instant of the tissue rupture using a pressure transducer (N5901; Nihon Denki Sanei, Tokyo, Japan).

The elastic modulus of the biotubes was examined using a custom designed tensile tester. Tubular samples were cut circumferentially and opened. Tissue specimens, 10 × 10 mm^2, were tested under humid conditions. The load was recorded until the samples ruptured, with a tissue-extension rate of 0.05 mm/s. Elastic modulus values were obtained from the maximum slope of the deformation-force relationships.

Measurement of the connective strength between leaflet and stent of the stent-biovalve was performed by use of a uniaxial tensile-testing apparatus (Rheoner II; Yamaden, Tokyo, Japan) [Figure 3]. The connective strength between native aortic valve and conduit of goat were also measured in same way. Each sample was fixed in a sample folder that was specially designed by use of a 3D printer (Projet HD3000; 3D Systems, Rock Hill, SC). The testing speed was 0.05 mm/s until failure, that is, tissue rupture. Ultimate tensile strength was calculated from the stress-strain curves.

In vitro valve function

Valve function was examined using a pulsatile circulation circuit (LaboHeart NCVC, IWAKI; working fluid, 0.9% saline; mean arterial pressure, 100 mmHg; mean flow rate, 5–6 L/min, Figure 4). The flow rate, left ventricular pressure, and aortic pressure were measured using an ultrasonic flow meter and pressure meter. The regurgitant ratio and mean flow rate at every 10 bpm from 70 to 120 pulsatile rates were evaluated.

RESULTS

Preparation of stent-biovalves

The two different sized assembled molds [outer diameter of stents, 14 or 20 mm; Figure 1(A)] that were embedded in the subcutaneous pouches of the beagle or the goat for 4 weeks showed complete encapsulation with autologous connective tissue [Figure 1(B)]. The implants could be easily harvested because the developed capsulated tissues and the surrounding subcutaneous tissues were connected only by very fragile, irregular, and redundant tissues, which could be easily removed. The capsulated tissues were dissected to remain the tissue for the leaflets [Figure 1(C)]. The molds could be smoothly removed from both ends of the implant because there was no adhesion between the molds and the tissues covering the stent [Figure 1(D)]. The leaflet tissues were strongly fixed at the three commissures. The stents were iced and then inverted inside out. The tissue flaps, which originally existed outside the stent, were thereby converted to inner leaflets; the stent-biovalves were thus completely prepared [Figure 1(E)]. During the inversion, no or little damage occurred to the leaflet tissues and to the connecting tissues between the leaflet and the stent. Two sized stent-biovalves with a sufficient coaptation area were thus obtained with outer diameter of 14 mm from beagles or 20 mm from goats [Figure 2]. The success rate of the stent-biovalve preparation was 100% (8/8) for each size.

The histological photographs showed that the valve leaflets of the stent-biovalve mainly consisted of collagen fibers [Figure 5]. The wall thickness of the valve leaflet was 285 ± 96.2 μm.

Mechanical properties

The burst strength of the leaflets of the stent-biovalves was over 7600 mmHg, which was closed to that of aortic valve leaflets (6200 ± 1400 mmHg).[16] Elastic modulus of the leaflets of the stent-biovalve was 2.6 ± 1.1 MPa, whereas that of goat aortic valve leaflets was 1.1 ± 0.4 MPa. To evaluate the

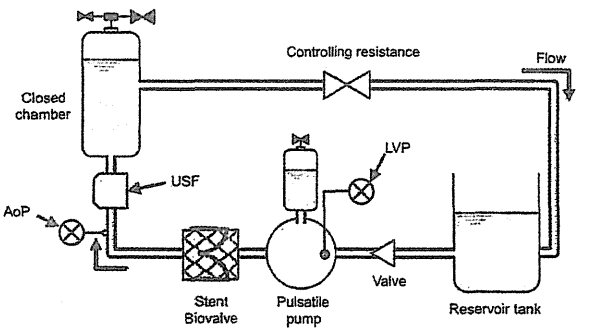

FIGURE 4. A pulsatile circulation circuit model designed for the evaluation of valve function. [Color figure can be viewed in the online issue, which is available at wileyonlinelibrary.com.]

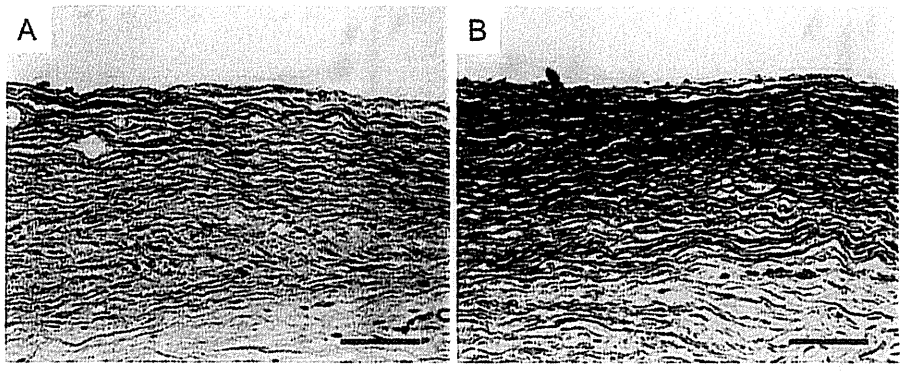

FIGURE 5. Histology of the leaflet of stent-biovalve stained with Hematoxylin and eosin staining (A) and Masson's and trichrome staining (B). bar = 100 μm. [Color figure can be viewed in the online issue, which is available at wileyonlinelibrary.com.]

connective strength between biovalve leaflet and stent, the tensile strength of the biovalve leaflet and stent was measured by using specially designed sample folder [Figure 5]. The connective strength between biovalve leaflets and stent was comparable to between aortic valve and conduit of goats. The mean values of ultimate tensile strength in each sample were as follows, biovalve leaflet-stent: 833.8 ± 215.5 gf; aortic valve-conduit of goat: 949.7 ± 186.1 gf.

In vitro valve function

The movement of the leaflets in a pulsatile flow circuit [Figure 4] was examined using videography. The stent-biovalve leaflets closed rapidly and tightly in synchronization with the backward flow in the diastolic phase. In the transition phase of the flow direction, the valve opened smoothly and the aperture ratio of the valve was 89% [Figure 6(A)], and coaptation of valve leaflets was optimal [Figure 6(B)].

Figure 6(C) shows the flow rate waveforms of the stent-biovalve at 70 bpm. Regurgitation in the diastolic phase was almost completely prevented. The mean flow rate was ~5–6 L/min [Figure 7(A)], and the regurgitation ratio was ~4% for each heart rate tested [Figure 7(B)].

DISCUSSION

Here, we report the successful development of novel construction method for a stent-biovalve with robust valve leaflets and favorable *in vitro* function. In the previously reported design for biovalves, the molds were designed such that valve leaflets were formed by connective tissue penetrating the apertures in the preparation molds. However, such tissue ingrowth was slow; the formation of the valve leaflets therefore required a long duration and was not always robust.

In this technique, the structure of the new molds for the stent-biovalve ensured successful formation of three valve leaflets, with broad flaps available. The key point of this mold design was that the outer circumferential connective tissue was used to form each valve leaflet. Typically, in a trileaflet valve with a diameter of 14 mm, the horizontal leaflet length for adequate coaptation in the closed valve is 14 mm. Using this method, the leaflet was formed along the acrylic cylinder-shaped part, which had a length of 17 mm, on the outer side of the stent that had a diameter of 14 mm. Thus, the formed leaflet had a length of 17 mm, which is ~1.2 times longer than that required for definitive coaptation. Since the area of the leaflet tissues was sufficient large, an extremely low regurgitation rate (~4%) was noted when testing *in vitro* valvular function, much lower than that noted for the previous biovalve (type IV, regurgitation rate 20%).

Moreover, since the valve leaflets were technically formed in the opening state, each valve leaflet opened smoothly in the systolic phase, resulting in a high aperture ratio of 89%. In addition, the leaflet tissues were very

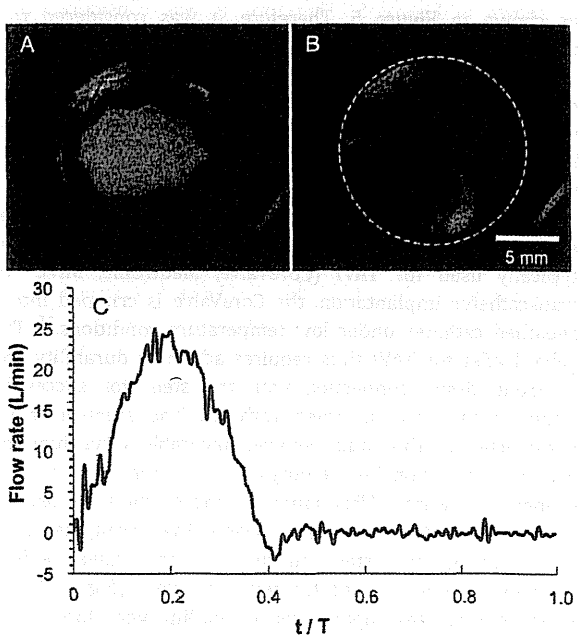

FIGURE 6. Macroscopic photos of the opening (A) and closing (B) form of the stent-biovalve in the circuit as shown in Figure 3. The pulsatile flow was 70 bpm, and the mean flow rate was 5–6 L/min. The aperture ratio was 89%. Pulsatile flow waveform in a single cycle of the stent-biovalve. [Color figure can be viewed in the online issue, which is available at wileyonlinelibrary.com.]

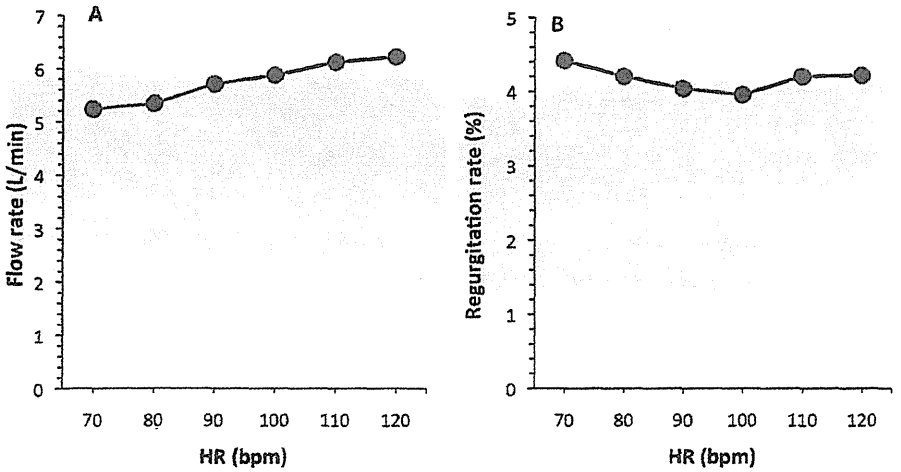

FIGURE 7. Mean flow rate (A) and regurgitation rate (B) at every 10 bpm from 70 to 120 bpm.

robust because the tissues were originally formed as a conduit. The burst strength of the leaflets of the stent-biovalve was over 7600 mmHg, which was about 2 times larger than that of canine pulmonary valve leaflets (3600 ± 780 mmHg) and over that of aortic valve leaflets (6200 ± 1400 mmHg).[16] In addition, elastic modulus of the leaflets of the stent-biovalve was 2.6 ± 1.1 MPa, which was over 2 times larger than that of goat aortic valve leaflets (1.1 ± 0.4 MPa). The cells in the leaflet tissue of the stent-biovalve were rare as shown in Figure 5. Therefore, it was considered that there was little influence of cells in the biomechanics. The connective strength between biovalve leaflet and stent was comparable to native aortic valve and conduit. Therefore, we believe strongly that the robust properties of valve leaflets of the stent-biovalve were demonstrated by these mechanical results.

To facilitate the use of the stent-biovalve in TAVI, a self-expandable nitinol stent was chosen in this study, which is typically used for TAVI (CoreValve, Medtronic, MN). For transcatheter implantation, the CoreValve is crimped into a sheathed catheter under low temperature conditions.[18] The valve leaflet for TAVI thus requires adequate durability and a strong tissue connection with the stent for successful crimping into the sheathed catheter. The stent-biovalves constructed in this study showed favorable valve function even after eversion (inside out) under low temperature conditions (iced water). This handling exposed the valve leaflets to conditions that were more severe than crimping. Even after turning the stent inside out, the valve leaflets remained strongly connected with the stent [Figure 1(D)], which did not tear apart even by pulling with forceps, as demonstrated in the type IV biovalve, which was strongly attached to a scaffold material.[14] Therefore, it is highly expected that the valve leaflets of the stent-biovalve would have sufficient durability and a robust tissue connection with the stent for crimping into a sheathed catheter for TAVI.

Because the biovalve is an engineered tissue, it will have to maintain its function in living bodies, and the living body would be the best environment for testing the biovalve. Therefore, we believe that there is little value in examining the long-term durability of the biovalve in an *in vitro* system. However, in separate study, we evaluated the durability of the biovalve in *in-vitro* pulsatile flow of saline.[19] Even after biovalve pulsated more than four million times (heart rate = 70 bpm; mean flow rate = 5.0 L/min; mean aortic pressure = 92 mm Hg), stable continuous operation was possible without excessive reduction of the flow rate or bursting. However, in our recent report, postoperative echocardiography showed smooth movement of the leaflets of the biovalve with little regurgitation under systemic circulation (2.6 ± 1.1 L/min) at least for 2 months of implantation to goat in an apico-aortic bypass model.[17] Therefore, we believe that the stent-biovalve has similar excellent durability in *in vitro* and *in vivo*.

Recently, several studies reported that tissue engineered valved stents were successfully implanted as pulmonic valve *in vivo*.[20–23] These materials may overcome the limitations of bioprosthetic heart valve prostheses and may be expected further evolution to be applied to clinical use. However, these tissue-engineered valved stents require complicated cell management protocols with cell culture under strictly sterile conditions, and also require decellularized allografts or synthetic scaffold materials to seed autologous cells. In this study, autologous heart valve with stent (stent-biovalve) showed favorable valve function, without expensive facilities or complicated manipulations. Stent-biovalve may overcome the limitations of bioprosthetic heart valve prostheses and have the advantage of other tissue engineered valved stents.

In this study, the pulsatile circuit was designed for actual human aortic valve conditions (mean flow = 5 L/min; mean pressure = 100 mmHg; heart rate = 70–100 bpm); however, saline solution was selected as a working fluid. The kinetic viscosity of blood is 4.4×10^{-6} m^2/s, which is

~4 times that of saline solution (1.0×10^{-6} m^2/s). Thus, our circuit did not approximate the viscosity of blood; however, it was considered that the present design achieved an adequate performance of valvular function for a future animal implantation study. We do not have any additional data on the biomechanics of the tissue affected after long-term stress. However, this is our near future research topics. We are now planning implantation study of the stent-biovalve to beagle dogs. However, we previously reported that in the tissue of the biotube, which was also obtained by IBTA technology from rod molds, the elastic modulus value of the biotube after implantation was 2× higher than that of the native arteries. The biotube after implantation acquired further robust property of maintenance of the preimplantation elongation ability.

Based on the American College of Cardiology/American Heart Association valvular guidelines 2006,[2] the regurgitant fraction of the present stent-biovalve was much lower than the "mild" classification, in fact being present at "trace" levels. Yare et al. reported that 75% of bioprosthetic valves used for TAVI showed trace to mild aortic regurgitation (AR) after implantation; however, such AR did not affect LV structure and function.[24] Previous biovalves were demonstrated to have favorable valve function and histological changes when used as heart valves in a beagle model[14]; further, biotubes created by IBTA technology regenerated arteries within 3 months of implantation.[25] Therefore, although this evaluation of the stent-biovalve was performed *in vitro*, it is expected that this stent-biovalve with autologous valve leaflets will show more favorable function *in vivo* than *in vitro*. We expect that this stent-biovalve could eventually be applied for TAVI, with favorable valve function *in vivo*.

CONCLUSION

We successfully developed a novel method for efficient construction of a robust, completely autologous heart valve eversion of a self-expandable stent, and named the resulting product the stent-biovalve. These stent-biovalves were obtained after only 4 weeks of subcutaneous embedding in a beagle dog or a goat. Owing to the large and robust leaflet tissues that were developed in the open-form position, excellent *in vitro* valve function was achieved. Future studies are expected to focus on the implantation of this stent-biovalve in animal models to confirm chronic valve function and durability *in vivo*.

REFERENCES

1. Iung B, Baron G, Butchart EG, Delahaye F, Gohlke-Bärwolf C, Levang OW, Tornos P, Vanoverschelde JL, Vermeer F, Boersma E, Ravaud P, Vahanian A. A prospective survey of patients with valvular heart disease in Europe: The Euro Heart Survey on Valvular Heart Disease. Eur Heart J 2003;24:1231–1243.
2. Bonow RO, Carabello BA, Chatterjee K, de Leon AC Jr, Faxon DP, Freed MD, Gaasch WH, Lytle BW, Nishimura RA, O'Gara PT, O'Rourke RA, Otto CM, Shah PM, Shanewise JS, Smith SC Jr, Jacobs AK, Adams CD, Anderson JL, Antman EM, Fuster V, Halperin JL, Hiratzka LF, Hunt SA, Lytle BW, Nishimura R, Page RL, Riegel B. ACC/AHA 2006 guidelines for the management of patients with valvular heart disease: A report of the American College of Cardiology/American Heart Association Task Force on Practice Guidelines (writing committee to revise the 1998 Guidelines for the Management of Patients With Valvular Heart Disease). J Am Coll Cardiol 2006;48:e1–148.
3. Iivanainen AM, Lindroos M, Tilvis R, Heikkilä J, Kupari M. Natural history of aortic valve stenosis of varying severity in the elderly. Am J Cardiol 1996;78:97–101.
4. Le Tourneau T, Savoye C, McFadden EP, Grandmougin D, Carton HF, Hennequin JL, Dubar A, Fayad G, Warembourg H. Mid-term comparative follow-up after aortic valve replacement with Carpentier-Edwards and Pericarbon pericardial prostheses. Circulation 1999;100(19 Suppl):II11–16.
5. Cribier A, Eltchaninoff H, Bash A, Borenstein N, Tron C, Bauer F, Derumeaux G, Anselme F, Laborde F, Leon MB. Percutaneous transcatheter implantation of an aortic valve prosthesis for calcific aortic stenosis: First human case description. Circulation 2002; 106:3006–3008.
6. Latib A, Maisano F, Bertoldi L, Giacomini A, Shannon J, Cioni M, Ielasi A, Figini F, Tagaki K, Franco A, Covello RD, Grimaldi A, Spagnolo P, Buchannan GL, Carlino M, Chieffo A, Montorfano M, Alfieri O, Colombo A. Transcatheter vs surgical aortic valve replacement in intermediate-surgical-risk patients with aortic stenosis: A propensity score-matched case-control study. Am Heart J 2012;164:910–917.
7. Bloomfield P, Wheatley DJ, Prescott RJ, Miller HC. Twelve-year comparison of a Bjork-Shiley mechanical heart valve with porcine bioprostheses. N Engl J Med 1991;324:573–579.
8. Hammermeister K, Sethi GK, Henderson WG, Grover FL, Oprian C, Rahimtoola SH. Outcomes 15 years after valve replacement with a mechanical versus a bioprosthetic valve: Final report of the Veterans Affairs randomized trial. J Am Coll Cardiol 2000;36:1152–1158.
9. Emmert MY, Weber B, Wolint P, Behr L, Sammut S, Frauenfelder T, Frese L, Scherman J, Brokopp CE, Templin C, Grünenfelder J, Zünd G, Falk V, Hoerstrup SP. Stem cell-based transcatheter aortic valve implantation: First experiences in a pre-clinical model. JACC Cardiovasc Interv 2012;5:874–883.
10. Metzner A, Stock UA, Iino K, Fischer G, Huemme T, Boldt J, Braesen JH, Bein B, Renner J, Cremer J, Lutter G. Percutaneous pulmonary valve replacement: Autologous tissue-engineered valved stents. Cardiovasc Res 2010;88:453–461.
11. Nakayama Y, Ishibashi-Ueda H, Takamizawa K. In vivo tissue-engineered small-caliber arterial graft prosthesis consisting of autologous tissue (biotube). Cell Transplant 2004;13:439–449.
12. Hayashida K, Kanda K, Yaku H, Ando J, Nakayama Y. Development of an in vivo tissue-engineered, autologous heart valve (the biovalve): Preparation of a prototype model. J Thorac Cardiovasc Surg 2007;134:152–159.
13. Hayashida K, Kanda K, Oie T, Okamoto Y, Ishibashi-Ueda H, Onoyama M, Tajikawa T, Ohba K, Yaku H, Nakayama Y. Architecture of an in vivo-tissue engineered autologous conduit "Biovalve". J Biomed Mater Res B Appl Biomater 2008;86:1–8.
14. Yamanami M, Yahata Y, Tajikawa T, Ohba K, Watanabe T, Kanda K, Yaku H, Nakayama Y. Preparation of in-vivo tissue-engineered valved conduit with the sinus of Valsalva (type IV biovalve). J Artif Organs 2010;13:106–112.
15. Nakayama Y, Yahata Y, Yamanami M, Tajikawa T, Ohba K, Kanda K, Yaku H. A completely autologous valved conduit prepared in the open form of trileaflets (type VI biovalve): mold design and valve function in vitro. J Biomed Mater Res B Appl Biomater 2011;99:135–141.
16. Yamanami M, Yahata Y, Uechi M, Fujiwara M, Ishibashi-Ueda H, Kanda K, Watanabe T, Tajikawa T, Ohba K, Yaku H, Nakayama Y. Development of a completely autologous valved conduit with the sinus of Valsalva using in-body tissue architecture technology: A pilot study in pulmonary valve replacement in a beagle model. Circulation 2010;122 (11 Suppl):S100–106.
17. Takewa Y, Yamanami M, Kishimoto Y, Arakawa M, Kanda K, Matsui Y, Oie T, Ishibashi-Ueda H, Tajikawa T, Ohba K, Yaku H, Taenaka Y, Tatsumi E, Nakayama Y. In vivo evaluation of an in-body, tissue-engineered, completely autologous valved conduit (biovalve type VI) as an aortic valve in a goat model. J Artif Organs 2012;16:176–184.

18. Grube E, Laborde JC, Gerckens U, Felderhoff T, Sauren B, Buellesfeld L, Mueller R, Menichelli M, Schmidt T, Zickmann B, Iversen S, Stone GW. Percutaneous implantation of the CoreValve self-expanding valve prosthesis in high-risk patients with aortic valve disease: The Siegburg first-in-man study. Circulation 2006; 114:1616–1624.
19. Sumikura H, Nakayama Y, Ohnuma K, Takewa Y, Tatsumi Y. In vitro evaluation of a novel autologous aortic valve (Biovalve) with a pulsatile circulation circuit. Artif Organs. Forthcoming.
20. Weber B, Scherman J, Emmert MY, Gruenenfelder J, Verbeek R, Bracher M, Black M, Kortsmit J, Franz T, Schoenauer R, Baumgartner L, Brokopp C, Agarkova I, Wolint P, Zund G, Falk V, Zilla P, Hoerstrup SP. Injectable living marrow stromal cell-based autologous tissue engineered heart valves: First experiences with a one-step intervention in primates. Eur Heart J 2011;32:2830–2840.
21. Schmidt D, Dijkman PE, Driessen-Mol A, Stenger R, Mariani C, Puolakka A, Rissanen M, Deichmann T, Odermatt B, Weber B, Emmert MY, Zund G, Baaijens FP, Hoerstrup SP. Minimally-invasive implantation of living tissue engineered heart valves: A comprehensive approach from autologous vascular cells to stem cells. J Am Coll Cardiol. 2010;56:510–520.
22. Metzner A, Stock UA, Iino K, Fischer G, Huemme T, Boldt J, Braesen JH, Bein B, Renner J, Cremer J, Lutter G. Percutaneous pulmonary valve replacement: autologous tissue-engineered valved stents. Cardiovasc Res 2010;88:453–461.
23. Lutter G, Metzner A, Jahnke T, Bombien R, Boldt J, Iino K, Cremer J, Stock UA. Percutaneous tissue-engineered pulmonary valved stent implantation. Ann Thorac Surg 2010;89:259–263.
24. Yared K, Garcia-Camarero T, Fernandez-Friera L, Llano M, Durst R, Reddy AA, O'Neill WW, Picard MH. Impact of aortic regurgitation after transcatheter aortic valve implantation: Results from the REVIVAL trial. JACC Cardiovasc Imaging 2012;5:469–477.
25. Watanabe T, Huang H, Hayashida K, Okamoto Y, Nemoto Y, Kanda K, Yaku H, Nakayama Y. Development of small-caliber "Biotube" vascular grafts: Preliminary animal implantation study. Artif Organs 2005;29:733.

[医薬品医療機器レギュラトリーサイエンス，PMDRS，44(4)，328～334 (2013)]

SERIES 医療機器をめぐる現状と展望 (40)

医療・診断機器をNICE(英国医療技術評価機構)はどう評価するか

妙中 義之[*1]，ミレラ・マーロウ[*2]，稲垣 悦子[*1]

How NICE (National Institute for Health and Clinical Excellence) Evaluates Medical Technologies

Yoshiyuki TAENAKA[*1], Mirella MARLOW[*2] and Etsuko INAGAKI[*1]

1. はじめに

医療機器を開発，市場に導入する際には，その国での薬事的な認可を取得することと同じように市場に出す際の価格の戦略も重要である．

欧米主要国(米国，英国，ドイツ，フランス)における保険収載・償還制度は，ケースペイメント(診断群別包括支払い)とそれを補完する仕組みからなる．新製品や新技術導入においても暫定的な保険償還を得ながら臨床現場に届けて，エビデンスに基づいて通常の償還プロセスにつなげられるいくつかのパスウェイが用意されている．また，いずれの国においても医療技術評価機関が存在している[1]．Table 1に示すように，主要国の保険制度では新技術や新製品導入への制度的な工夫がなされている[1]．

英国では，英国市場参入や普及に重要な役割を担う英国医療技術評価機構(NICE: National Institute for Health and Clinical Excellence)という組織があり，新規性の高い医療・診断機器については，ここで医療経済的評価をし，優位性の高い製品が普及するように医療機関へ推奨するという仕組みがある．

『「英国に学ぶ医療機器ビジネス」セミナー ～英国のヘルスケア政策と英国医療技術評価機構(NICE)の役割～』(英国総領事館，大阪商工会議所主催)が2012年12月6日に開催され，その中で，NICE医療技術評価センター医療機器・診断システムプログラム部長ミレラ・マーロウ女史(Mrs. Mirella Marlow, Programme Director, Devices and Diagnostic Systems, Centre for Health Technology Evaluation, National Institute for Health and Clinical Excellence (NICE))による「医療・診断機器をNICEはどう評価するか」の講演があった．

本稿はその講演内容を紹介するものである．

2. NICEと医療・診断機器

2.1 NICEとは

NICE (www.nice.org.uk)は，英国国民医療サービス(NHS: National Health Service)内の独立組織として1999年に国立臨床評価機構(National Institute for Clinical Excellence)として設立され，2005年にHealth Development Agencyを併合して現在のNational Institute for Hearth and Clinical Excellenceとなった(2012年の健康・社会福祉法制定(Health and Social Care Act 2012)を受け2013年4月1日以降，NICEの体制が変更となり，独立行政法人(NDPB: Non Department Public Body) the National Institute for Health and Care Excellenceとなる(通称は現行通りNICEを使用)．

[*1] 独立行政法人 国立循環器病研究センター，研究開発基盤センター 大阪府吹田市藤白台5-7-1(〒565-8565)
National Cerebral and Cardiovascular Center, 5-7-1 Fujishiro-dai, Suita, Osaka 565-8565, Japan
[*2] 英国医療技術評価機構(NICE)医療技術評価センター
Devices and Diagnostic Systems, Centre for Health Technology Evaluation, National Institute for Health and Clinical Excellence (NICE), 1st Floor 10 Spring Gardens, London, SW1A 2BU

[注] 本稿のFig. 1～10及びTable 2～7はNational Institute for Health and Clinical Excellence (NICE)からいただいたスライドから作成したものであり，改めてそのご厚意に感謝申し上げます．

Table 1　主要国の保険制度では新技術や新製品導入への制度的な工夫がなされている[1)]

	日本	英国	フランス	ドイツ	米国
償還の方式	・個別の治療手技，医薬品，材料ごと ・治療ケース（DPC：入院の場合の一部）	治療ケースごとの支払い	・入院の場合は治療ケースごとの支払い ・治療や処置ごと	・入院の場合は治療ケースごとの支払い ・治療や処置ごと	治療ケースごとの支払い
公定価格の有無	手技，薬剤，材料などは公定価格	入院，外来ともなし	植込みデバイス，外来診療などはあり	入院はなし 外来はあり	入院，外来ともなし
公的償還制度の運営主体	国．皆保険制度として全国一律	地域，地方ごと	地域，地方ごと	地域，地方ごと	連邦の制度に加えて地域，地方ごと
新技術や新製品への償還手続き	薬価や材料価格の申請と中医協での審査	地域，地方での機関との交渉を重ねたうえで中央審議	地方自治体，病院の経営主体との協議を重ねて中央審議	NUB	地域，地方での機関との交渉を重ねたうえで中央審議
医療技術評価機関（HTA）	公的機関なし	NICE	CNEDiMTS CEPS UNCAM CHAP	DIMDI/IQWIG/InEK	CMS 民間機関

NICE は疾病や健康障害の予防，診断，治療に最も効果的な方法について，独立の立場から，エビデンスに基づく信頼性のあるガイダンスを公表し，医療の公平性と一貫性を担保している．NICE ガイダンスは，最良な品質のケアを提供し，コストパフォーマンスの最大化を図るべく医療従事者等を支援することを目的としており，NHS，地方自治体，慈善団体等の医療，公衆衛生，ソーシャルケアのサービス委託者，提供者が対象であり，NICE はこれらの組織がガイダンスを実践するための支援も行っている．

1999 年，NICE 設立当時は技術評価プログラム（TAP: Technology Appraisals Programme）ただ一つのみであり，最初に公表したガイダンスは「親不知の抜歯」であったが，2012 年には NICE が公表したガイダンスは様々な製品及びサービスに影響を及ぼすようになってきている（Fig. 1）．

2012 年現在，予算は 6,380 万ポンドあり，スタッフ数 563 名，オフィスをロンドン，マンチェスター，リバプールに置いており，医療・診断機器に関連するガイダンスに関しては Health Technology Evaluation の部門が担当し（Fig. 2），科学的な厳格さをガイダンスの基本理念として

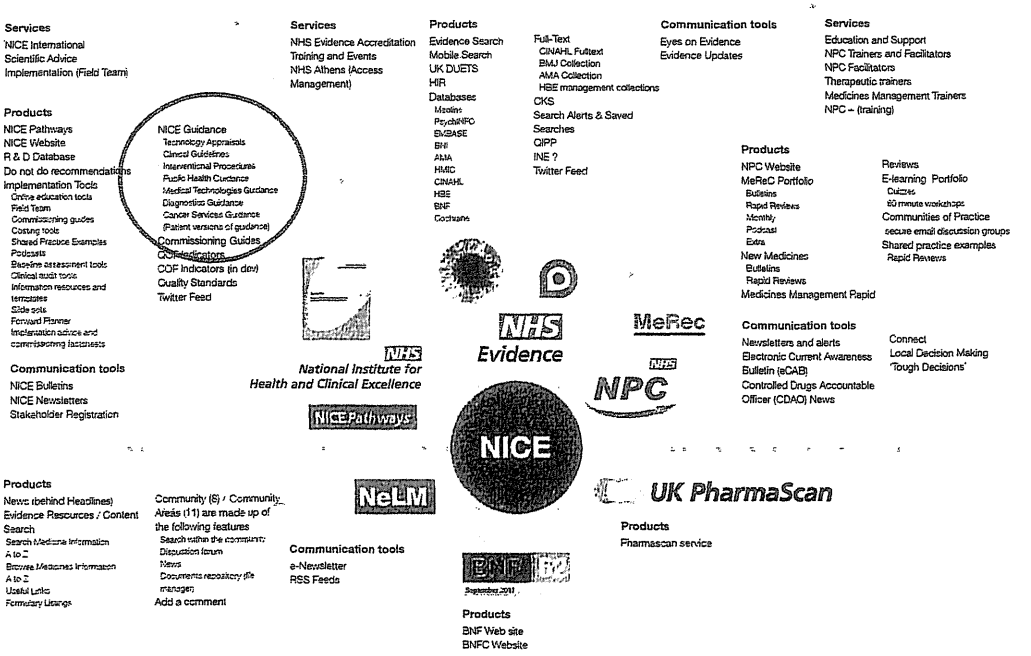

Fig. 1　2012　NICE Products & Services

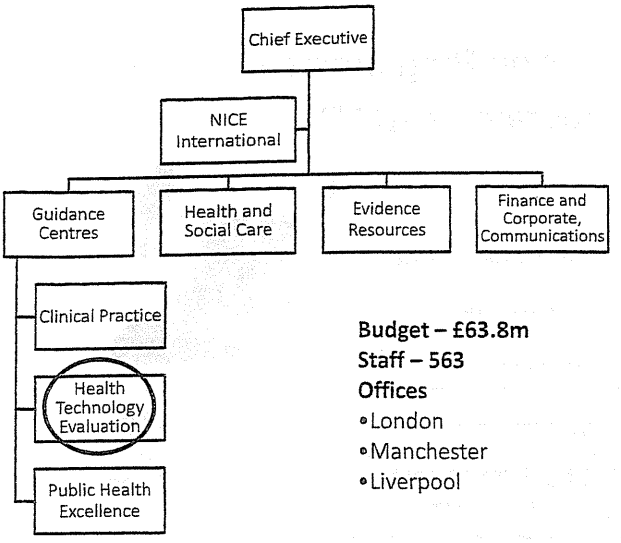

Fig.2 NICE in 2012

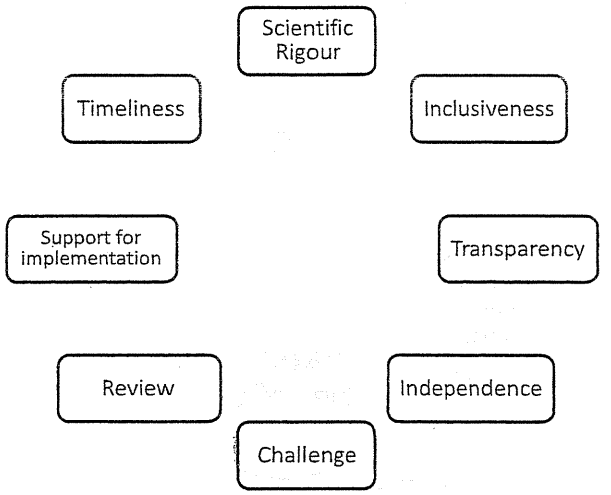

Fig.3 NICE Guidance Principles

いる (Fig. 3).

2.2 Next Stage Review (通称 "Darzi Report") June 2008 (Table 2)

2008年，現役医師でもある保健省政務次官のダルジ卿は就任後1年をかけ英国医療改革の成果と現状を総点検し，今後の改革の方向性を示すため，包括的なレビュー（政策の点検・見直し）"High Quality Care For All"（すべての人々に質の高いケアを）を発表した．この改革レビューの重要なメッセージは「量 (Quantity) から質 (Quality) へ」の転換であり，今後10年間の改革の方向性を示すものであった．

これまでの英国の医療改革は主に「量」の側面に着目した改革が多く，一定の成果を挙げたことを評価した上で，

Table 2 Next Stage Review ("Darzi Report") June 2008

- New treatments are constantly redefining what high quality care looks like. We must support innovation to foster a pioneering NHS.
- For new medical technologies, we will simplify the pathway by which they pass from development into wider use, and develop ways to benchmark and monitor uptake.

これからは医療の「質」の側面に力を入れていく，というブラウン政権の宣言といえる．これにより，NICE の予算は3倍に増え，ガイダンス発行までの審査期間の短縮を図るため，NICE の機能強化が実施された[2]．

2.3 NICE の新しい医療技術評価プログラム (Fig. 4)

NICE は2009年と2010年に2つの新しいプログラム，医療技術評価プログラム (MTEP: Medical Technologies Evaluation Programme) と診断技術評価プログラム (DAP: Diagnostics Assessment Programme) を立ち上げた．これらのプログラムは革新的な医療機器や診断技術の医療経済的評価を目的としており，そのねらいは：

・NHS に新しい医療技術の採用を促す．

・民間及び NHS の共同研究を活性化し，評価対象技術の臨床上又は／及び医療システム全体への便益に係るエビデンスを収集蓄積する．

である．

NICE は，医療・診断機器は医薬品とは異なる然るべき方法で評価されるべきであるとの認識の下，MTEP，DAP プログラムを始めた．革新的な医療機器は医療システムや患者に対して様々な利益をもたらすが，往々にして医療機器は医薬品に比べて，エビデンスの整備が遅れているからである．また購買に高額な投資が必要なため導入が難しい製品もある．NICE は医療機器及び診断技術のガイダンス策定を通じて，NHS が製品の価値を適正に判断できるようにするための支援を行っている (Fig. 5, 6, Table 3).

2.4 医療技術プログラムの評価対象となる製品

医療技術プログラムの対象となる製品は，埋込み型医療機器等の治療用機器，患者の自立を助ける医療技術，症状を発見しモニターするための診断機器や試験等である．対象製品は，下記の欧州法規に定めるものである：

・医療機器：Medical Devices Directive (MDD) -93/42/EEC

・能動埋込型医療機器：Active Implantable Medical Devices Directive (AMDD) - 90/385/EEC

・体外診断用医療機器：In-Vitro Diagnostics Directive (IVDD) - 98/79/EC